ISSN 2472-1972

Cytogenetic, Genomic, and Functional Characterization of Pituitary Gonadotrope Cell Lines

Frederique Ruf-Zamojski,[1] Yongchao Ge,[1] Hanna Pincas,[1] Jidong Shan,[2] Yinghui Song,[2] Nika Hines,[3] Kevin Kelley,[3] Cristina Montagna,[2] Pranav Nair,[1] Chirine Toufaily,[4] Daniel J. Bernard,[4] Pamela L. Mellon,[5] Venugopalan Nair,[1] Judith L. Turgeon,[6] and Stuart C. Sealfon[1,7]

[1]Department of Neurology, Center for Advanced Research on Diagnostic Assays, Icahn School of Medicine at Mount Sinai, New York, New York 10029; [2]Molecular Cytogenetic Core, Albert Einstein College of Medicine, New York, New York 10461; [3]Mouse Genetics and Gene Targeting CoRE, Icahn School of Medicine at Mount Sinai, New York, New York 10029; [4]Department of Pharmacology and Therapeutics, McGill University, Montreal, Quebec, H3G 1Y6, Canada; [5]Department of Obstetrics, Gynecology and Reproductive Sciences, University of California San Diego, La Jolla, California 92093; [6]Department of Internal Medicine, University of California Davis, Davis, California 95616; and [7]Department of Neuroscience, Friedman Brain Institute, Icahn School of Medicine at Mount Sinai, New York, New York 10029

ORCiD numbers: 0000-0002-2451-8598 (F. Ruf-Zamojski); 0000-0003-2343-5851 (C. Montagna); 0000-0002-8856-0410 (P. L. Mellon); 0000-0001-5791-1217 (S. C. Sealfon).

LβT2 and αT3-1 are important, widely studied cell line models for the pituitary gonadotropes that were generated by targeted tumorigenesis in transgenic mice. LβT2 cells are more mature gonadotrope precursors than αT3-1 cells. Microsatellite authentication patterns, chromosomal characteristics, and their intercellular variation have not been reported. We performed microsatellite and cytogenetic analysis of both cell types at early passage numbers. Short tandem repeat (STR) profiling was consistent with a mixed C57BL/6J × BALB/cJ genetic background, with distinct patterns for each cell type. Spectral karyotyping in αT3-1 cells revealed cell-to-cell variation in chromosome composition and pseudodiploidy. In LβT2 cells, chromosome counting and karyotyping demonstrated pseudotriploidy and high chromosomal variation among cells. Chromosome copy number variation was confirmed by single-cell DNA sequencing. Chromosomal compositions were consistent with a male sex for αT3-1 and a female sex for LβT2 cells. Among LβT2 stocks used in multiple laboratories, we detected two genetically similar but distinguishable lines via STR authentication, LβT2a and LβT2b. The two lines differed in morphological appearance, with LβT2a having significantly smaller cell and nucleus areas. Analysis of immediate early gene and gonadotropin subunit gene expression revealed variations in basal expression and responses to continuous and pulsatile GnRH stimulation. LβT2a showed higher basal levels of *Egr1*, *Fos*, and *Lhb* but lower *Fos* induction. *Fshb* induction reached significance only in LβT2b cells. Our study highlights the heterogeneity in gonadotrope cell line genomes and provides reference STR authentication patterns that can be monitored to improve experimental reproducibility and facilitate comparisons of results within and across laboratories.

Freeform/Key Words: gonadotrope cell lines, LβT2, STR profiling, karyotyping, SC DNA sequencing, transcriptional response to GnRH

Abbreviations: CN, copy number; Ct, cycle threshold; DAPI, 4′,6-diamidino-2-phenylindole; FBS, fetal bovine serum; HBSS, Hanks balanced salt solution; ISMMS, Icahn School of Medicine at Mount Sinai; qPCR, quantitative polymerase chain reaction; SC, single cell; SKY, spectral karyotyping; SNV, single-nucleotide variant; STR, short tandem repeat.

Received 14 February 2019
Accepted 8 March 2019
First Published Online 25 March 2019

For several decades, the αT3-1 [1] and LβT2 [2] gonadotrope cell lines have been important cell model systems for the study of signaling and regulatory responses [3–9]. Both cell lines were generated by targeted oncogenesis in transgenic mice. αT3-1 cells were derived from a pituitary tumor in a mouse carrying the promoter region of the human glycoprotein α subunit linked to the SV40 T antigen oncogene [10]. LβT2 cells originated from a pituitary tumor in a mouse carrying the rat LHβ regulatory region fused to the same oncogene [11]. Although αT3-1 cells express *Cga* and *Gnrhr* and respond to GnRH with increased *Cga* transcript levels [10], LβT2 cells additionally express *Lhb* and induce *Fshb* gene expression in response to activin A or GnRH [12–14]. Moreover, in response to pulsatile GnRH stimulation, LβT2 cells increase *Lhb* and *Gnrhr* gene expression and secrete LH [11, 15, 16]. Thus, although αT3-1 cells represent an earlier embryonic stage of cell differentiation in the gonadotrope lineage, LβT2 cells are phenotypically more mature gonadotropes (for review, see [17]).

The importance of cell line authentication to improve experimental reproducibility across laboratories has been increasingly recognized and required by funding agencies and academic journals [18, 19]. Authentication of human cell lines is typically achieved by assaying microsatellite short tandem repeats (STRs) [20]. However, most mouse cell lines, such as αT3-1 and LβT2, do not have reference STR patterns. To facilitate authentication, we determined the STR patterns in early passage αT3-1 and LβT2 cells. We present a cytogenetic characterization of the αT3-1 and LβT2 cells and evaluate relative copy number (CN) changes throughout the LβT2 genome using single-cell (SC) whole genome sequencing. Authentication discriminated two LβT2 cell lines that were compared morphologically and functionally.

1. Materials and Methods

A. Cell Culture and Treatment

GnRH was purchased from Bachem (Torrance, CA). All LβT2 and αT3-1 cell stocks originated from Dr. Pamela Mellon (University of California, San Diego, CA). Cells were cultured at 37°C in DMEM (Mediatech, Herndon, VA) supplemented with 10% fetal bovine serum (FBS; Gemini, Calabasas, CA) in a humidified air atmosphere of 5% CO_2. Cells were frozen in freezing medium containing 70% DMEM, 20% FBS, and 10% dimethyl sulfoxide (Sigma, St. Louis, MO) and maintained in liquid nitrogen.

For continuous GnRH stimulation experiments, LβT2 cells were seeded in 12-well plates at 350,000 cells per well in 10% FBS-supplemented medium. For immediate early gene expression measurements, after 2 days of culture cells were treated with either vehicle or 2 nM GnRH in 10% FBS-supplemented medium for different time periods. For gonadotropin subunit expression measurements, after 1 day of culture, cells were incubated overnight in low-serum (1% FBS) medium (day 2) and then treated with either vehicle or 2 nM GnRH in low-serum medium for 2 hours, followed by 4 hours in the absence of GnRH (day 3). For each condition/time point, a minimum of four biological replicates (*i.e.,* independent wells) were collected.

For pulsatile GnRH stimulation experiments, LβT2 cells were seeded on glass poly-D-lysine–coated coverslips (#GG-24-PDL; Neuvitro, Vancouver, WA) at 750,000 cells per coverslip and cultured in 10% FBS-supplemented medium. After 1 day of culture, coverslips were placed in racks and incubated overnight in low-serum (1% FBS) medium (day 2). On day 3, cells were exposed to 5-minute duration pulses of 2 nM GnRH every 2 hours (a frequency that is more favorable to *Fshb* induction than to *Lhb*) in low-serum medium, and temporal gene responses were assessed after the fourth or fifth pulse, as previously described [21, 22]. For each time point, a minimum of four biological replicates (*i.e.,* independent coverslips) were collected. Experiments comparing LβT2a and LβT2b lines were conducted in parallel.

B. Cell Line Authentication

For αT3-1 cells, an early passage (p7) aliquot of cells provided by Dr. Mellon was used for authentication. For LβT2 cells, cell line authentication occurred every 3 to 6 months and was

achieved by comparing our cells with an early passage (p10) aliquot of the LβT2 cells isolated by Dr. Mellon in 1996. Frozen aliquots of cells were shipped to Idexx BioResearch (Columbia, MO) for cell line authentication. The *CellCheck Mouse Plus* profile performed by Idexx includes (i) cell line identification by STR DNA profiling and (ii) multiplex PCR-based interspecies contamination check for the mouse, rat, human, Chinese hamster, and African green monkey. STR profiling was performed using either 27 dinucleotide repeats or nine tetranucleotide repeats. The tetranucleotide STR profile has been reported to provide more discrimination between cell lines than the 27 marker–based profile [23].

C. Chromosome Harvesting and Counting

LβT2 metaphase specimens were prepared by the Mouse Genetics and Gene Targeting CoRE at the Icahn School of Medicine at Mount Sinai (ISMMS) according to standard cytogenetic procedures for cultured cells [24]. Briefly, cell division was blocked at the metaphase stage by adding the spindle poison vinblastine (#V1377, Sigma) for 3 hours. Following trypsinization (#25-052-Cl, Corning, Corning, NY), cells were incubated in a hypotonic solution for 15 minutes (which makes the cell swell, thus allowing easy rupture of the cell membrane) and preserved in a swollen state with Carnoy's fixative solution (methanol/glacial acetic acid 3:1; methanol, #650609, Sigma; acetic acid, #A6283, Sigma). Chromosome spreads were prepared by dropping fixed cell suspensions from a height onto cold slides, completely drying the slides, and staining them in a Giemsa-staining solution (#89002, Thermo Fisher Scientific, Waltham, MA). Chromosome counting was done manually using an inverted microscope at 600× magnification by visualizing Giemsa-stained chromosome spreads on a monitor. Plastic was overlaid on the monitor, and chromosomes were marked one by one with a Sharpie; after the marks were wiped clean, chromosomes in the next cell were counted. Chromosomes were counted in at least 20 cells.

D. Karyotyping

D-1. Metaphase preparation

Briefly, cells were split 1 day before harvest for obtaining metaphase chromosomes. Colcemid (#15210-040, Gibco, Thermo Fisher Scientific) was added at a final concentration of 0.1 μg/mL. Cells were incubated at 37°C for 30 minutes before being washed and trypsinized. After a short centrifuge step, the cell pellet was resuspended in 0.075 M KCl and incubated at 37°C for 15 to 25 minutes. The reaction was stopped by adding a few drops of fixative (methyl alcohol/glacial acetic acid, 3:1; methyl alcohol, #A433P-4, Fisher Scientific, Hampton, NH; glacial acetic acid, #A38-212, Fisher Scientific). Cells were pelleted and resuspended in fresh fixative. Slides were prepared afterward.

D-2. G-banding

Trypsin (#0152-13, Sigma) was used to denature euchromatic histones in DNA regions with higher transcriptional activity. Following Giemsa staining, these regions appear as light bands. Conversely, highly condensed DNA regions (heterochromatin) with little or no transcriptional activity have a large portion of their histones protected from the trypsin and will therefore stain darkly following Giemsa staining. Briefly, slides were immersed into a 0.5% trypsin solution in 1× Hanks balanced salt solution (HBSS; #14170-112, Gibco, Thermo Fisher Scientific) for 5 seconds, then rinsed in HBSS only before being placed in HBSS and FBS (#900-208, Gemini Bio-Products, West Sacramento, CA) for 30 seconds and quickly rinsed again in HBSS. Giemsa solution was prepared fresh (3:1 ratio of Gurr Buffer and Giemsa stain, #2375-0078, EM Diagnostic System, Fisher Scientific), and slides were incubated in this solution for 5 minutes. Following wash steps, slides were mounted in Permaslip Mounting Medium and Liquid Coverslip (Alban Scientific Inc., St. Louis, MO), and imaged under a light microscope.

D-3. Spectral karyotyping

DNA spectral karyotyping (SKY) hybridization was performed as previously described [25] with commercial SKY paint probes from Applied Spectral Imaging (Carlsbad, CA). Briefly, slides were washed in Earl's medium, incubated in a trypsin/EDTA solution, washed in water, and dehydrated in an increasing ethanol series (70%, 80%, 100% ethanol). Chromosome denaturation was performed by placing the slides in 2× SSC for 2 minutes, then dehydrating them in an ethanol series. Denaturation solution was heated to 72°C in a glass Coplin jar, and slides were placed in the solution for 1.5 minutes before being immediately placed in a cold ethanol series. Spectral Karyotyping Reagent (Applied Spectral Imaging) was heated to 37°C and added to the denatured chromosome preparation. Following a 24- to 36-hour incubation at 37°C in a humidified chamber, the slides were washed in 0.4× SSC at 72°C for 2 minutes. The slides were next washed in a 4× SSC/0.1% Tween 20 solution for 1 minute, the fluid was drained, and Cy5 staining reagent was added for 40 minutes at 37°C. Following an ultimate wash, the slides were mounted with antifade 4′,6-diamidino-2-phenylindole (DAPI) reagent and readied for spectral imaging. Rearrangements are defined with nomenclature rules from the International Committee on Standard Genetic Nomenclature for Mice [26].

E. SC DNA Amplification and Sequencing

SCs were picked into 2.5 μL of PBS using the CellRaft (Cell Microsystems, Research Triangle Park, NC) SC picking system, following the manufacturer's guidelines. DNA amplification was performed using the Rubicon Genomics PicoPLEX WGA Kit (cat #R30050) with the adjustment of final amplification cycles to eight following the manufacturer's instructions. Purification was carried out using AMPure beads at a 0.9× concentration. Following amplification, 300 ng of DNA was used to create Ion Torrent libraries using the NEBNext Fast DNA Fragmentation & Library Prep Set for Ion Torrent (cat #E6285L) with a few minor modifications. The adapter ligation was completed with 3 μL of NEXTflex® DNA Barcodes (cat #NOVA-401004), and the final amplification step was omitted. After the libraries were purified using AMPure beads, 250-bp fragments were size-selected with the Invitrogen E-gel size selection system (Carlsbad, CA). The libraries were sequenced at an average of 0.2× coverage on the Ion Proton.

F. Quantification and Quality Control of DNA and Libraries

DNA quality and quantity were determined with Quant-iT PicoGreen dsDNA Reagent (Invitrogen) using a fluorescence microplate reader (SpectraMax M3; Molecular Devices, Sunnyvale, CA). Library quantification and quality control were evaluated using Nanodrop, Qubit (fluorometric quantitation; Thermo Fisher Scientific, Waltham, MA), Kapa (quantification; Kapa Biosystems, Wilmington, MA), and the High-Sensitivity DNA Bioanalyzer assay (Agilent, Santa Clara, CA) and quantitative real-time PCR for selected test genes.

G. SC DNA Sequencing Data Analysis

Sequences were aligned to the mm10 mouse genome using the Torrent Suite 5.2.2 software. The SC DNA-seq data are deposited in the Sequence Read Archive database (Sequence Read Archive accession: PRJNA521776). CN variation analysis is based on the HMMcopy method, as described in [27], with customized R script.

H. Cell Staining and Imaging

Cells from each LβT2 line were seeded on poly-D-lysine–treated coverslips at about 100,000 cells per coverslip, cultured in DMEM supplemented with 10% FBS, and incubated at 37°C for 24 hours in a humidified air atmosphere of 5% CO_2. After being washed with 1× PBS, coverslips were immersed in the staining solution containing 10 μL of CellMask Orange

Plasma Membrane Stain stock (C10045; Molecular Probes, Eugene, OR) in 1× PBS at 37°C for 10 minutes. After removal of the staining solution by aspiration, coverslips were washed once with 1× PBS, and cells were fixed with warm 4% paraformaldehyde (prepared from a 16% solution; #5710-S; Electron Microscopy Sciences, Hatfield, PA) at 37°C for 10 minutes. Coverslips were then washed once with 1× PBS and incubated in a 300 nM DAPI solution (cat #D1306; Thermo Fisher Scientific) for 5 minutes at room temperature. Coverslips were rinsed twice with 1× PBS and once with water before being mounted on glass slides using Prolong Gold antifade reagent (cat #P10144; Invitrogen, Eugene, OR) and sealed with clear nail polish. Epifluorescent microscopy was performed on both an Olympus BX60 microscope equipped with a BX-FLA Reflected Light Fluorescence Attachment and a CCD-based image analysis system and a Zeiss Axio Imager Z2 microscope operated with the Zen Pro software, using magnifications of 40× (air) and 63× (oil). The imaging filters on the Zeiss microscope were for DAPI AT350/50× (excitation)/T400LP (Beam Split)/ET460/50 m (Emission) and for Cell Mask Orange ET560/40× (excitation)/T585LPXR (Beam split)/ET630/75 m (Emission).

I. Imaging Analysis

Analysis was performed using Image J 1.48v [28]. For cell area measurements, cells were manually segmented in Image J, and cell areas were recorded. For nucleus area measurements, images were automatically segmented using the routine provided by the Melbourne Advanced Microscopy Facility (www.microscopy.unimelb.edu.au; routine by Cameron Nowell). Nucleus areas were automatically quantified and the spreadsheet exported in Excel. Any nuclei detected with less than 10 pixels were considered debris or dust particles and were excluded from the analysis. Each imaging analysis was done on an independent slide holding two coverslips (one for each cell line). In two experiments, measurements were separately acquired by two observers for independent confirmation. All data were exported and analyzed using GraphPad Prism [29] statistical software package version 5.04.

J. Quantitative Real-Time PCR

Quantitative real-time PCR experiments were performed as previously described [30]. Following total RNA isolation, 1 μg of RNA was reverse-transcribed with the Affinity Script reverse-transcriptase (Agilent). Next, samples were diluted 1:20 in molecular biology-grade H_2O (Cellgro, Manassas, VA). SYBR Green quantitative polymerase chain reaction (qPCR) assays were performed (40 cycles) in an ABI Prism 7900HT thermal cycler (Applied Biosystems, Foster City, CA) using 5 μL of cDNA template and 5 μL of master mix containing the specific primers for the targeted gene, Platinum®Taq DNA polymerase, and the required qPCR buffer, following the manufacturer's recommendations. Three technical qPCR replicates were run for each biological replicate. Results were exported as cycle threshold (Ct) values, and Ct values of target genes were normalized to that of *Rps11* in a subsequent analysis. Data were expressed as arbitrary units by using the formula $E = 2500 \times 1.93^{(\text{rps11 Ct value} - \text{gene of interest Ct value})}$, where E is the expression level in arbitrary units. Primer sequences were previously described [22, 31].

K. Statistical Analysis

Statistical calculations were performed using GraphPad Prism. Statistical significance was assessed by the *t* test and is indicated in the figure legends.

2. Results

A. Authentication of αT3-1 and LβT2 Cell Lines by STR Genotyping

Cell lines were authenticated using two types of STR profiling: one with a panel of 27 dinucleotide repeats, the other with a newer nine-tetranucleotide repeat panel showing higher specificity [23]. STR profiles of the *α*T3-1 and L*β*T2 cell lines were compared with those

of C57BL/6J and BALB/cJ mice. The cell lines were derived from matings of CB6F1/J mice, which are a cross between C57BL/6J and BALB/cJ mice [10, 11]. Interspecies contamination tests were conducted to exclude any cellular contamination from rat or human samples.

A-1. αT3-1 cell line

Within the 27-marker panel, the majority of markers (74%) corresponded to the genotype of either C57BL/6J mice, BALB/cJ mice, or CB6F1/J hybrid mice (Table 1). Most of the markers

Table 1. Genetic Profiling of αT3-1 and LβT2 Cell Lines

A	2-nt Repeat Marker	Chromosome	Fragment Size (bp)				
			αT3-1 Cells	LβT2 Cell Stock 1	LβT2 Cell Stock 2	C57BL/6J Mice	BALB/cJ Mice
	4	1	156, 164	156, 170	156, 170	156	160
	5	2	127	113	113	113	127
	136	2	161	149	149	149	160
	78	3	197, 202	202	202	197	202
	134	3	104	111	111	112	104
	14	4	95, 104	95	95	95	105
	94	5	113	113	113	113	111
	16	5	136	136, 143	136, 143	136	143
	139	5	106, 121	106, 121	106, 121	121	106
	144	6	207	208	207	193	211
	25	6	137	137	137	141	137
	133	7	77	82	81	82	78
	138	7	186	191	191	191	182
	163	7	240	219	219	219	242
	27	8	150, 163	163	163	151	165
	39	9	157, 174	157, 174	157, 174	173	157
	165	10	197	197	197	197	191
	141	10	95, 118	95	95	95	114
	74	11	102, 119	102, 119	102, 119	119	102
	111	11	148	148	148	148	144
	20	12	155	155	155	153	155
	31	13	167	167, 198	167	198	167
	137	14	203	204	204	204	209
	143	14	136, 144	132	132	133	137
	53	15	96	96	96	96	82
	171	16	216	210, 216	210, 216	210	216
	47	19	119	119	119	114	119

B	4-nt Repeat Marker	Chromosome	Repeat Number				
			αT3-1 Cells	LβT2 Cell Stock 1	LβT2 Cell Stock 2	C57BL/6J Mice	BALB/cJ Mice
	MCA-4-2	4	20.3, 21.3	20.3, 21.3	20.3, 21.3	20.3	21.3
	MCA-5-5	5	14, 17	13, 17	13, 17	17	14
	MCA-6-4	6	18	19	19, 20	18	17
	MCA-6-7	6	12	12	12	17, 18	12
	MCA-9-2	9	15, 18	18	18	18	15
	MCA-12-1	12	16	16, 17	16, 17	17	16
	MCA-15-3[a]	15	21.3	22.3	22.3	22.3	22.3
	MCA-18-3	18	16, 17	16, 17	16, 17	16	18
	MCA-X-1	X	28, 29	25	25	27	24

The genotypes of the αT3-1 cell line and two LβT2 cell stocks were compared with those of C57BL/6J and BALB/cJ mice. STR profiles were generated using either (Table 1A) a panel of 27 dinucleotide repeat-based markers or (Table 1B) a panel of nine tetranucleotide repeat-based markers. In Table 1A, an allele call is presented as the fragment size (in bp) of a PCR product obtained at a particular locus. Note that a 1-bp difference in fragment size between the αT3-1 sample and one of the comparison profiles represents only run-to-run variability. In Table 1B, an allele call is presented as the number of repeats detected at a particular locus.

[a]The marker is uninformative between mouse strains.

that exhibited a homozygous allele distribution (15 of 18) matched with the genotype of either C57BL/6J or BALB/cJ mice. Within the nine-marker panel, 89% of markers matched the genotype of either C57BL/6J, BALB/cJ, or CB6F1/J mice. One of the nine markers, located on the X chromosome, was heterozygous, and only one allele matched with the C57BL/6J strain. Overall, STR profiling was consistent with a mixed background, with C57BL/6J and BALB/cJ as the main strains of origin. No interspecies contamination was detected.

A-2. LβT2 cell line

When testing our LβT2 cell stocks, we discovered two distinct LβT2 genotypes, which are investigated further in the following text. In the LβT2a cell stock, more than 88% of the markers within the 27-marker panel corresponded to the genotype of either C57BL/6J mice, BALB/cJ mice, or CB6F1/J hybrid mice (Table 1). The majority of markers (20 of 27) had a homozygous allele distribution, with only two showing an unexpected fragment size. In the nine-marker panel, all markers matched with the genotype of either C57BL/6J, BALB/cJ, or CB6F1/J mice. Globally, the genetic profile of LβT2 cells was consonant with a mixed background, with C57BL/6J and BALB/cJ as the main strains of origin. Interspecies contamination tests were negative.

A second LβT2 cell stock (LβT2b) has been used in our laboratory as well as in other laboratories. Although its authentication pattern was similar to that of the first LβT2 cell stock evaluated, its genotype was clearly distinguishable (see Table 1). Thus, these represent two genetically distinguishable lines, LβT2a and LβT2b. Within the 27-marker panel, marker 31 presented the loss of an allele in LβT2b compared with the LβT2a line, which showed heterozygosity. Within the nine-marker panel, marker MCA-6-4 had an additional allele in LβT2b, in contrast with a homozygous allelic distribution in LβT2a. The morphology and functional responses of these two lines are compared in a later section.

B. Cytogenetic Maps of αT3-1 and LβT2a Cell Lines Reveal Aneuploidy

B–1. αT3-1 cell line

Although normal mouse cells are diploid (with 2N = 40 chromosomes), analysis of 10 metaphase spreads from αT3-1 cells revealed pseudodiploidy, with karyotypes ranging from 32,XO to 40,X. Chromosomal rearrangements were also observed (Fig. 1A; Table 2). Chromosomal translocations and deletions, as well as centromere duplications, were observed. Of note, translocation of a portion of chromosome 9 into chromosome 1 occurred in all cells analyzed, and part of sex chromosome Y was translocated in chromosome 6 in seven of 10 cells. The Y chromosome was intact in three cells. No two cells were identical. SKY analysis was consistent with a male mouse origin of the line.

B–2. LβT2a cell line

Chromosome counting in more than 20 cells from LβT2a cell stock at two different passages (Table 3) and G-banding karyotyping of five cells (Table 4) were concordant with pseudotriploidy (3N), with a composite karyotype of 47–72,XX. No two cells had identical karyotypes. Many intact chromosomes were present at three or four copies within one cell. Chromosomes 14, 16, and 17 showed a typically high duplication rate. Karyotype analysis also was most consistent with the LβT2 cells having a female origin. In addition, our reexamination of previous genome-wide transcriptome data in LβT2 cells [32] showed the absence of chromosome Y–expressed genes compared with male pituitaries. Further, our reanalysis of previous genome-wide chromatin accessibility data [30] provided evidence for the absence of the Y chromosome and the presence of two X chromosomes in comparison with autosome coverage. Therefore, three independent analyses converged toward a female origin for LβT2 cells. Multiple chromosomal aberrations were detected in different cells, especially gains of chromosomes, Robertsonian translocation of chromosome 4 [4], and one translocation

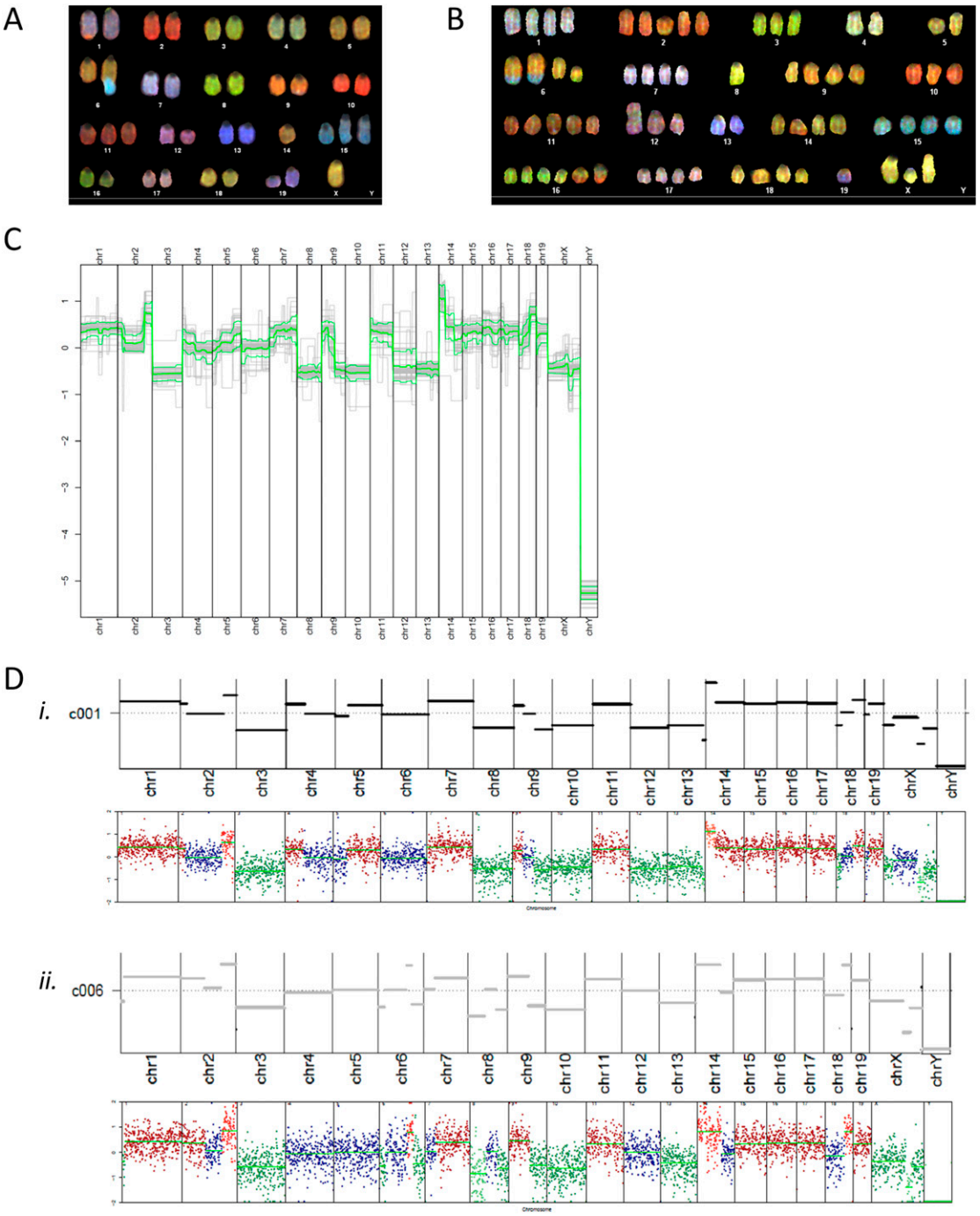

Figure 1. Spectral karyotyping of the αT3-1 and LβT2 cell lines and analysis of copy number variation in individual LβT2 cells. Colored karyotypes of (A) an αT3-1 and (B) an LβT2 cell from LβT2 cell stock were obtained using DNA spectral karyotyping hybridization. (C) Summary of SC copy number variation in all analyzed cells is shown. Relative CNs in log2 scale per chromosome are depicted. The thick green line signifies the average CN for all cells; the upper and lower thin green lines represent the SD. (D) SC copy number variation in two individual cells (*i* and *ii*) are shown: examples are c001 (in *i*) and c006 (in *ii*). The top panel, which corresponds to a single gray trace in (C), depicts relative CN in log2 scale, as derived from the HMMcopy algorithm. The bottom panel provides relative sequencing depth in log2 scale at each binned chromosome position. Bin size = 500,000 bp. Relative copy number and relative sequencing depth are winsorized to (−2, 2) [*i.e.,* data >2 (or less than −2) are converted to 2 (or −2) to allow better global data visualization]. The indicated chromosome numbers apply to both top and bottom panels.

Table 2. SKY Analysis Report for αT3-1 Cells

Cell	Cell 06-02	Cell 08-03	Cell 10-04	Cell 16-07	Cell 18-08	Cell 22-10	Cell 26-12	Cell 28-13	Cell 30-14	Cell 32-15
Chromosome no.	40,XO	35,XO	38,XO	38,XO	38,XO	32,XO	37,XY	37,XO	39,XY	39,XY
Chromosome 1	2, t [1, 9]	2, t [1, 9]	2, t [1, 9]	2, t [1, 9]	2, t [1, 9]	2, t [1, 9]	2, t [1, 9]	2, t [1, 9]	2, t [1, 9]	2, t [1, 9]
Chromosome 2	2	2	2	2	2	2	2	2	2	2
Chromosome 3	2	1	2	2	2	1	2	2	2	2
Chromosome 4	2	2	2	2	2	2	2	2	2, t [4, 5]	2
Chromosome 5	2	2	2	2	2	2	2	2	2	2
Chromosome 6	2, t(6;Y)	2, t(6;Y)	2, t(6;Y)	2, t(6;Y)	2, t(6;Y)	1	1	2, t(6;Y)	2	2, t(6;Y)
Chromosome 7	2	2	2	2	2	2	2	2	2	2
Chromosome 8	2	2	2	2	2	1	2	2	2	2
Chromosome 9	2	2	2	2	2	2	2	1	2	2, t [9, 1]
Chromosome 10	2	2	2	2	2	2	1	2, dup centromere	2	2
Chromosome 11	3, dup centromere	2	2	2	2	2	2	2, dup centromere	2	2
Chromosome 12	2, del [12]	2	3, del [12]	2, del [12]	2	2	1	2	2, del [12]	2, del [12]
Chromosome 13	2	2	2	2	2	2	2	2	2	2
Chromosome 14	1	1	1	1	1	1	1	1	1	1
Chromosome 15	3, del [15]	2	2	2	2	1	3, del [15]	2	3, del [15]	2
Chromosome 16	2	1	2	2	2	2	2	2	2	2
Chromosome 17	2	2	2	2	2	2	2	2	3	2
Chromosome 18	2	2	2	2	2	1	1	2	2	2
Chromosome 19	2	1	1	2	2, t [19, 15]	1	2	2	0	2, dup [19]
Chromosome X	1	1	1	1	1	1	1	1	1	1, t(X;?)
Chromosome Y	0	0	0	0	0	0	1	0	1	1

Spectral karyotyping was performed on 10 cells from the αT3-1 line, as described in the Materials and Methods section.
Abbreviations: ?, undetermined; del, deletion; dup, duplication; dup centromere, centromere duplication; t, translocation.

Table 3. Chromosome Counting in LβT2 Cells

	LβT2 Cell Stock 1	
Cell no.	**Passage p18**	**Passage p12**
1	66	66
2	68	66
3	66	66
4	66	67
5	64	64
6	64	66
7	66	63
8	66	60
9	64	65
10	65	67
11	65	64
12	65	65
13	66	66
14	66	65
15	65	64
16	66	66
17	66	66
18	72	66
19	66	67
20	68	65
21	72	
22	66	
23	66	
24	66	
25	64	
26	66	
27	66	

Chromosome counting was done in cells from LβT2 cell stock a, at two different passages (p18 and p12), as described in the Materials and Methods section.

[6, 15]. SKY analysis of 10 LβT2 cells complemented these findings (Fig. 1B; Table 5). Cells tended to be pseudotriploid, with a composite karyotype of 42–68,XX and frequent chromosomal rearrangements. Although all cells analyzed exhibited extra copies of chromosome 15, most of them also showed extra copies of chromosomes 2, 7, 14, 16, and 19. Chromosomal abnormalities occurred frequently and included deletions of (portions of) chromosomes, translocations, and Robertsonian translocations.

Globally, although both lines appeared to have comparable frequencies of chromosomal rearrangements (affecting chromosomal segments), LβT2a cells displayed a higher duplication rate of entire chromosomes than αT3-1 cells did, and thus a higher level of chromosomal instability.

C. SC Whole Genome Sequencing Confirms Chromosomal Variation Across Cells in the LβT2a Cell Line

To reliably identify genome-wide CN alterations in single LβT2 cells, we performed SC low-coverage DNA sequencing in 56 cells from LβT2 cell stock a. Analysis of the sequencing data obtained in the LβT2 cells indicated substantial cell-to-cell variability in relative CNs, as shown in Fig. 1C and 1D and in an online repository [33]. Across all LβT2 cells analyzed, chromosomes 1, 7, 11, and 14 to 19 and a portion of chromosome 9 tended to have higher CNs, which was generally consistent with the pattern of chromosomal gains observed in karyotype analyses. By contrast, chromosomes 3, 8, 10, 12, 13, and X and another part of chromosome 9 had lower CNs. The data also indicated the absence of a Y chromosome and the presence of X

Table 4. G-Banding Karyotyping of LβT2 Cells

Cell	Cell 02-19	Cell 02-18	Cell 02-04	Cell 02-21	Cell 02-02
Chromosome no.	61,XX	65,XX	53,XX	67,XX	47,XX
Chromosome 1	3	2	2	2	2
Chromosome 2	4	3	2	2	2
Chromosome 3	2	2	1	6	2
Chromosome 4	4, 1Rob [4]	2	2, 1Rob [4]	2, 1Rob [4]	2, 1Rob [4]
Chromosome 5	3	2	2	4	2
Chromosome 6	4	3	3	2	3, 1t [6, 15]
Chromosome 7	3	2	3	2	2
Chromosome 8	2	4	2	1	1
Chromosome 9	4	3	2	3	2
Chromosome 10	2	2	2	4	2
Chromosome 11	3	4	1	2	2
Chromosome 12	3	3	3	1	2
Chromosome 13	2	4	2	5	3
Chromosome 14	3	4	4	4	4
Chromosome 15	4	2	4	3	3
Chromosome 16	4	8	4	8	3
Chromosome 17	4	4	4	3	3
Chromosome 18	2	4	3	3	2
Chromosome 19	3	5	3	4	2
Chromosome X	2	2	2	2	2
Chromosome Y	0	0	0	0	0
Markers				4	1

G-banding karyotyping was carried out on five cells from LβT2 cell stock a, as described in the Materials and Methods section.
Abbreviations: Rob, Robertsonian translocation; t, translocation.

chromosomes in all individual cells studied, thus confirming karyotype analysis results. Overall, SC DNA sequencing confirmed the unbalanced number of chromosomes (3n+) and variable chromosomal aberrations observed by cytogenetics as well as provided an assessment of CN state.

D. LβT2a and LβT2b Lines Are Morphologically Distinct

We next compared the morphology of the two LβT2 lines. Cell shape and appearance were distinctive, as cells in LβT2b were larger, tended to have protrusions, and formed more angular foci than in LβT2a (Fig. 2A). Plasma membrane staining followed by image quantification revealed that the cell surface area was significantly wider in LβT2b than in LβT2a (Fig. 2B and [33]). Measurement of the nucleus area after nuclear staining showed that cells had significantly larger nuclei in LβT2b than in LβT2a in four of five experiments (Fig. 2B and [33]).

E. LβT2a and LβT2b Cells Exhibit Differences in Basal and GnRH-Induced Gene Expression

We next studied whether the two LβT2 lines showed differences in gene expression and response to GnRH. In experiments performed in parallel in both lines (LβT2a and LβT2b), we compared their patterns of immediate early gene and gonadotropin subunit gene expression and time course induction by GnRH under either continuous or pulsatile stimulation conditions (for details, see the Materials and Methods section). Both *Egr1* and *Fos* showed greater basal expression levels in LβT2a (Fig. 3A and 3B and [33]). Under continuous stimulation conditions, LβT2a showed more rapid induction of higher levels of *Egr1*. Conversely, *Fos* induction was significantly lower in LβT2a cells.

Table 5. SKY Analysis Report for LβT2 Cells

Cell	Cell 01-20	Cell 01-21	Cell 01-22	Cell 01-23	Cell 01-24	Cell 01-26	Cell 01-28	Cell 01-30	Cell 01-18	Cell 01-05
Chromosome no.	68,XXX	63,XX	59,XX	63,XXX	66,XX	49,XX	64,XX	55,XO	65,XX	42,XX
Chromosome 1	4	4	4	4	2	2	3	4	3	3
Chromosome 2	5, 1del(2)t [2, 6]	3	3	3	5, 1del [2] t [2, 6], 1t [2, 7]	4	3	4, 1del(2)t [2, 6]	5,1del(2)t [2, 6]	2
Chromosome 3	3	3, 1t [3, 11]	2	2	2	1	3	2	3	3
Chromosome 4	2	3	2, 1Rob [4]	2, 1Rob [4]	3, Rob [4]	1	3	2, Rob [4]	3	2
Chromosome 5	2	3	2	3, 1t [5, 14]	3	3	3	2	3	3
Chromosome 6	4, 2t [6, 15], 1del(6)t [6, 3]	4, 1del [6]	4	1	3	2	2	3	3	2
Chromosome 7	4	3	3, 1t [7, 10]	4, 1t [7, 15]	3	3	4	3, 1t [7, 2]	3	2
Chromosome 8	1	2	2	2	2	2	2	1	2	2
Chromosome 9	4	4	4	2	1	1	4	2	3	1
Chromosome 10	3	2	1	3, 1t [10, 17]	4, 1del [10]	2	3	4, 1del(10)t [10, 13]	2	2
Chromosome 11	5	3	4	3	5	3	2	4	3	1
Chromosome 12	3, 1Rob [12]	4	2	3	3, 1del [12]	2, 1Rob [12]	2	2	3	1
Chromosome 13	2	2	2	2	2	3	2	1	2	1
Chromosome 14	4, 1del [14]	4	5, 1t [14, 19]	3	3	3	3	2	3	2
Chromosome 15	4	4	3	6, 1del [15]	4	4	4	3	4	3
Chromosome 16	6, 2t [16, 2]	5, 1t [16, 2]	5, 2t [16, 2]	7, 2t [16, 2]	4	3, 2t [16, 2]	7, 1del [16], 2t [16, 2]	6, 2t [16, 2]	6, 2t [16, 2]	2
Chromosome 17	4	2	4	3	5	4	5	2	4	3
Chromosome 18	4	3	1	4	6	1	3	3	3	2
Chromosome 19	1	3	4	3	4	3	4	4	5	4
Chromosome X	3, 1del(X)	2	2	3	2	2	2	1	2	2
Chromosome Y	0	0	0	0	0	0	0	0	0	0

Spectral karyotyping was performed on 10 cells from LβT2 cell stock a, as described in the Materials and Methods section.
Abbreviations: del, deletion; Rob, Robertsonian translocation; t, translocation.

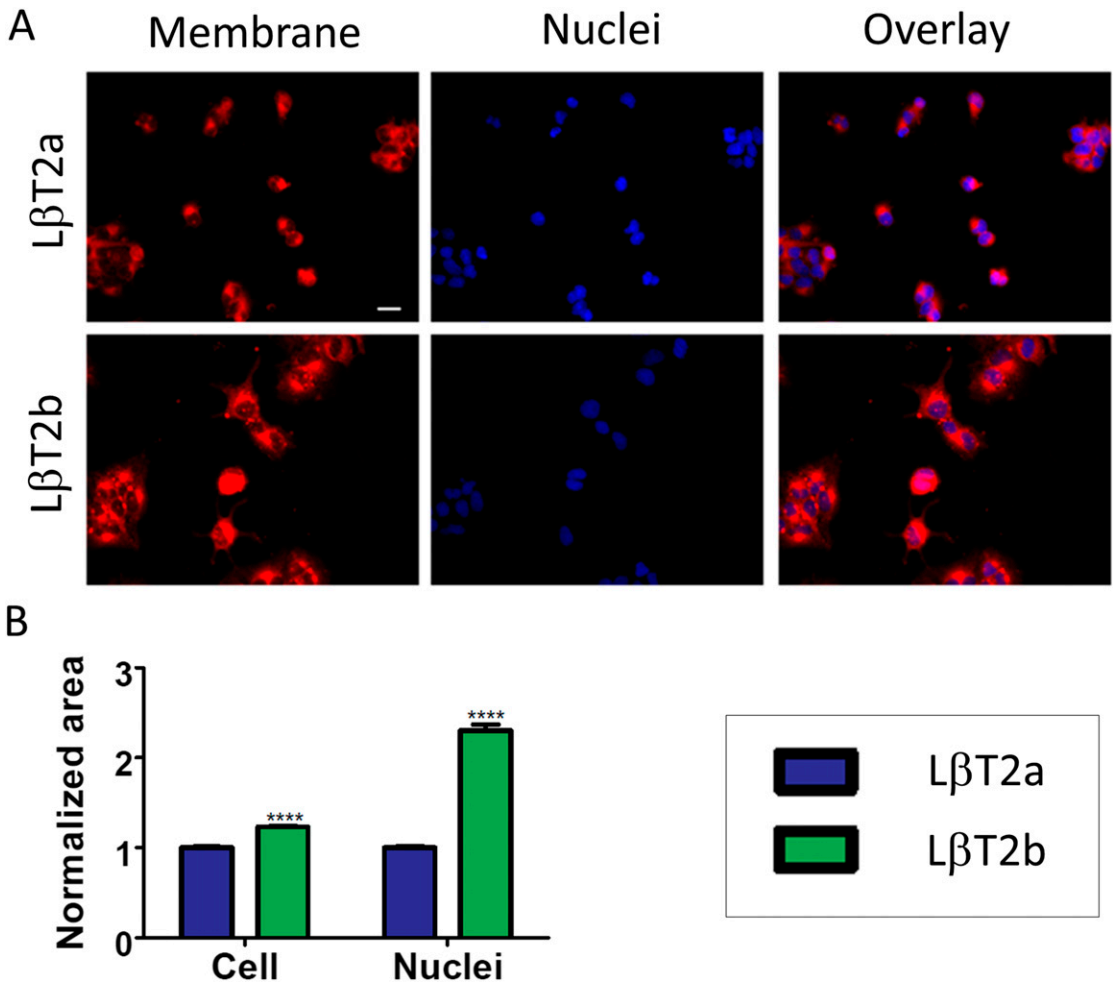

Figure 2. Two genetically distinct LβT2 lines have different morphological features. (A) Micrographs of cells from the LβT2a and LβT2b lines using plasma membrane dye CellMask (left panel) and nuclear stain DAPI (middle panel). An overlay of both membrane and nuclear staining is shown in the rightmost panels. (B) Cell area and nucleus area measurements obtained in LβT2a and LβT2b using ImageJ. Cell area measurements were acquired in 269 cells from LβT2a and 198 cells from LβT2b, and nucleus area measurements were acquired in 1656 cells from LβT2a and 2180 cells from LβT2b. Data shown are from one of five independent experiments. Scale bar is 20 μm. Bars show median ± SE (error bars). ****$P < 0.0001$.

Analysis of basal gonadotropin subunit gene expression revealed borderline detectable *Fshb* mRNA in both lines (Fig. 3C and [33]), which was consonant with previous studies [12, 14, 34]. *Lhb* basal transcript levels were significantly higher in LβT2a than in LβT2b. *Fshb* induction in response to continuous GnRH stimulation was not detected in LβT2a cells, whereas *Fshb* was significantly induced in LβT2b in two of three experiments (Fig. 3D and [33]). There was a nonsignificant trend toward induction of *Lhb* expression by GnRH in both lines (Fig. 3E and [33]).

With pulsatile GnRH stimulation for five pulses at 2 hour intervals, both *Egr1* and *Fos* showed the highest levels of expression 20 minutes after the last pulse and declined 40 minutes after the pulse, with the patterns being similar in both lines (Fig. 4A and [33]). These results were overall consistent with our previous observations [22]. However, the two lines showed differences in the intensity of gene responses to GnRH. In two of three experiments, *Egr1* induction at +20 minutes was significantly higher in LβT2a than in LβT2b, whereas *Fos* induction at +20 minutes was significantly higher in LβT2b and remained higher than

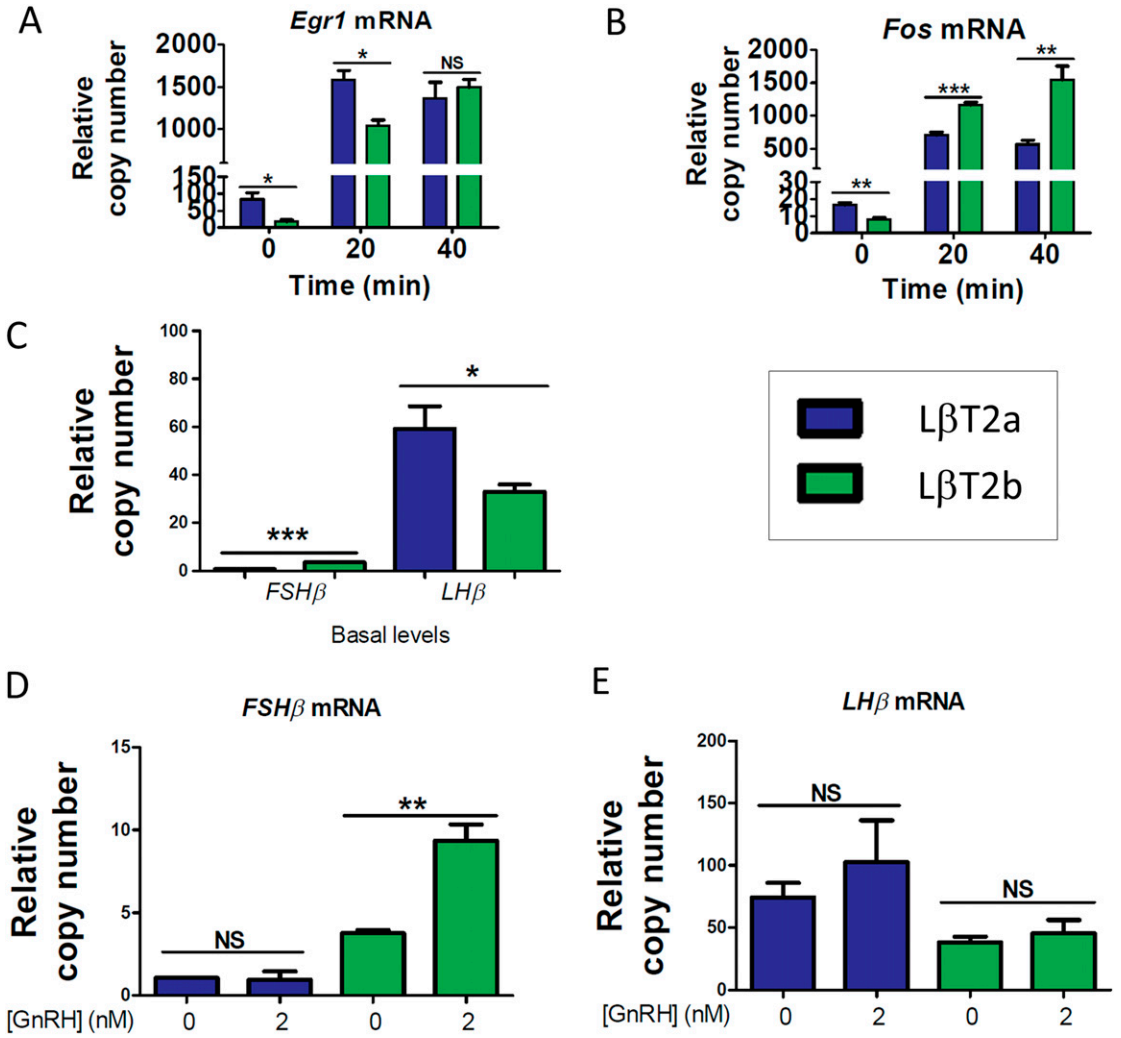

Figure 3. Two genetically distinct LβT2 lines show differences in immediate early gene and gonadotropin subunit gene expression and induction by GnRH. Time course of GnRH induction of (A) *Egr1* and (B) *Fos* in LβT2 cells (n = 6 biological replicates per time point). Gene expression was analyzed by qPCR. Cells were treated with 2 nM GnRH in 10% FBS medium for up to 40 min. (C) Basal expression of *Fshb* and *Lhb* is shown. (D) *Fshb* induction by GnRH is shown. (E) *Lhb* induction by GnRH in LβT2 cells (n = 4 biological replicates per condition) is shown. Gene expression was analyzed by qPCR. Following an overnight in a low-serum condition, cells were treated with 2 nM GnRH in a low-serum medium for 2 h, followed by 4 h in the absence of GnRH. Data shown are from one of three independent experiments. Bar graphs represent the median ± SE (error bars) of 4-6 biological replicates. $*P < 0.05$; $**P < 0.01$; $***P < 0.001$. NS, nonsignificant.

basal expression at +40 minutes in LβT2b. With respect to gonadotropin subunit gene expression, *Lhb* transcript levels increased in response to pulse stimulation in LβT2b in two of three experiments. However, although *Lhb* mRNA levels were comparable at all time points in LβT2a, they were significantly increased at +40 minutes in LβT2b (Fig. 4B, 4C and [33]). Although *Fshb* transcript levels did not show significant change over time in LβT2a, they gradually increased in LβT2b, reaching significance 40 minutes after the last pulse (Fig. 4B, 4C and [33]). This gradual increase was in keeping with the continuous increase of *Fshb* levels from pulse to pulse [22]. Overall, these results reveal differences in gene expression and response to GnRH between the two LβT2 lines, with the most notable difference being the divergence in *Fshb* induction by GnRH.

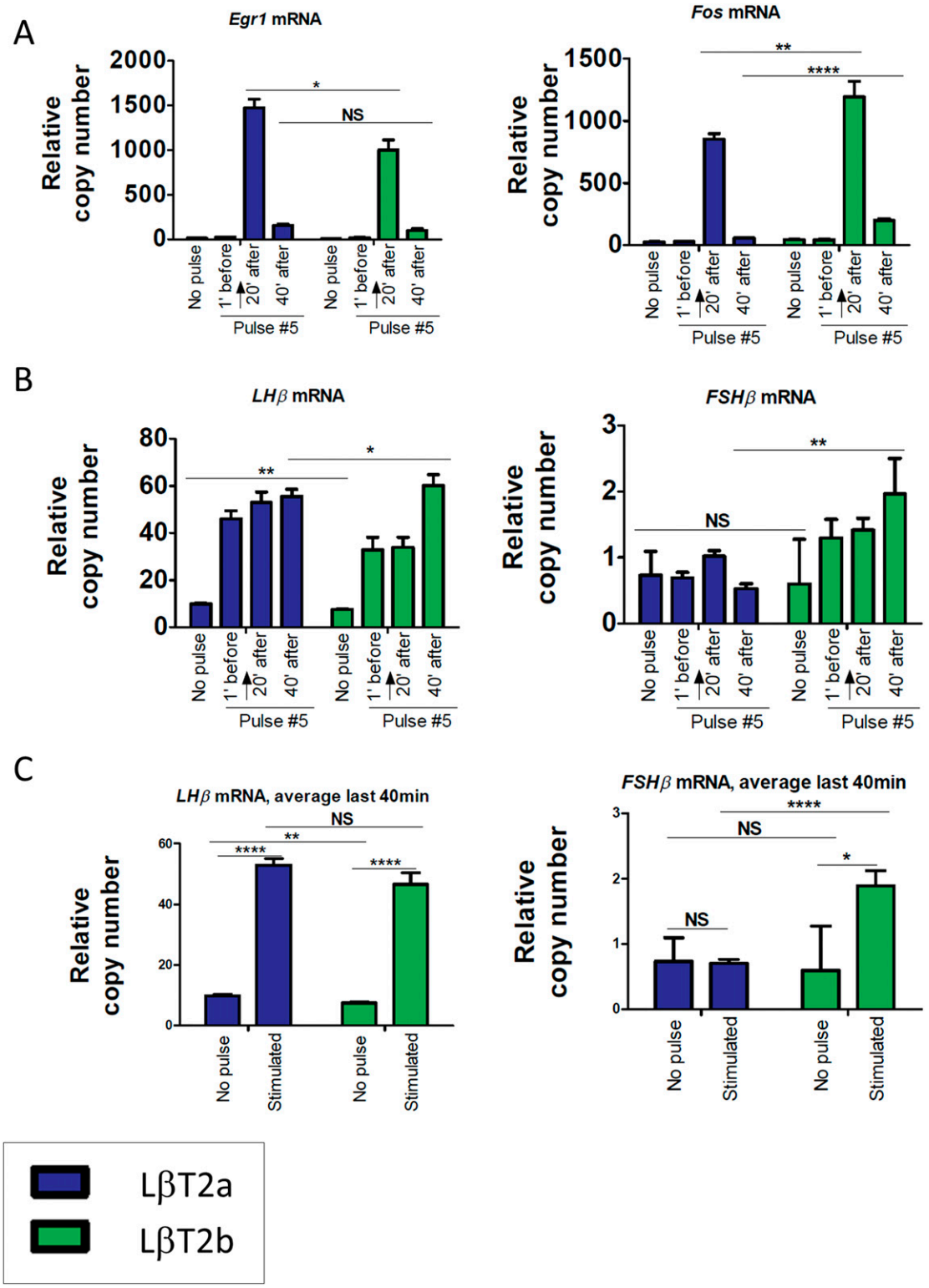

Figure 4. Two genetically distinct LβT2 lines show differences in temporal responses to GnRH pulse stimulation. Temporal responses of (A) *Egr1* and *Fos* and (B) *Lhb* and *Fshb* to GnRH pulse stimulation at low GnRH frequency are shown. (C) Average *Lhb* and *Fshb* responses over the last 40 min are shown. LβT2 cells were stimulated with 5-min pulses of 2 nM GnRH in a low-serum medium every 2 h for 8–10 h. Cells were harvested at short time intervals around the fifth pulse, as indicated. Arrows indicate the time of exposure to the GnRH pulse. Expression levels were determined by qPCR. Bar graphs represent the median ± SE (error bars) of six biological replicates. Data shown are from one of three independent experiments. $*P < 0.05$; $**P < 0.01$; $****P < 0.0001$. NS, nonsignificant.

3. Discussion

The establishment of the immortalized αT3-1 and LβT2 cell lines more than 2 decades ago has enabled researchers to examine the role of transcription factors involved in pituitary cell differentiation and in the transcriptional regulation of gonadotrope-specific genes. Moreover, it has facilitated the study of gene regulation by GnRH and feedback regulation of gonadotropins by endocrine mediators. Nevertheless, assessment of the cytogenetic and genomic characteristics of these cell lines has not been reported. Our results report the STR patterns of αT3-1 and LβT2 cells and identify two genetically, morphologically, and functionally distinct LβT2 lines. Our data are consistent with a male sex for αT3-1 cells and are most consistent with a female sex for LβT2 cells. We demonstrate that LβT2 and to a lesser extent αT3-1 cells show a high cell-to-cell variation in chromosome number and structure.

The genomic instability of these cell lines is consistent with the directed tumorigenesis in the mouse anterior pituitary used in their generation, and has been seen with other transgenic mouse cell line models created by targeted tumorigenesis [35–37]. Genomic instability in the αT3-1 and LβT2 cell lines was most likely induced by the SV40 T antigen. A 1997 study by Sargent *et al.* [38] showed that liver neoplasms isolated from transgenic rats harboring the albumin promoter–SV40 T antigen construct were aneuploid, with 70% of cells demonstrating duplication of all or part of chromosome 1 as the first karyotypic alteration, followed by loss of chromosomes 3, 6, and 15. The fact that the LβT2 line displays more chromosomal instability than the αT3-1 line (see Fig. 1A and 1B) could be partly related to the site of insertion of the SV40 T antigen oncogene in the mouse genome. It is tempting to speculate that insertion of the exogenous SV40 T antigen DNA into the mouse genome may have disrupted a gene encoding a key regulator of chromosome alignment during cell division. Further analysis is needed to identify potential candidate genes.

Interestingly, the murine LβT2 cell line shares some similarities with human pituitary cells immortalized with the SV40 T antigen. Cytogenetic analysis of the HP75 cell line, which was derived from human pituitary adenoma cells, and of the immortalized normal human pituitary CHP_2 cells revealed diploid and hypertetraploid cells with chromosomal abnormalities [39, 40]. Similar to the LβT2 cell line, the HP75 cell line expressed *LHB*, *CGA*, and *GnRHR* mRNAs but showed no FSH secretory response to GnRH (for FSH secretion in LβT2 cells, see [13]).

In the current study, we aimed to present the main chromosomal characteristics of an LβT2 cell line and to further evaluate the degree of cell-to cell variation using complementary cytogenetic and next-generation sequencing approaches. Of note, sequencing the genome of LβT2 cells at shallow depth restrained our ability to evaluate the nature and extent of chromosomal rearrangements, namely to identify structural variants (*i.e.,* deletions, duplications, inversions, and translocations) along the genome, assess the possibility of chromothripsis [41], detect single-nucleotide variants (SNVs) and loss of heterozygosity, and infer allelic variability and the potential effects of SNVs on protein function. Although obtaining high-depth sequencing data would allow us to extensively detect SNVs and structural variants in the LβT2 cell line and to discriminate major from minor structural aberrations, this would require additional experiments at a significantly higher cost and was beyond the scope of this report.

Given the genomic differences between the αT3-1 and LβT2 lines, one can assume that the CN state may influence gene expression levels in each line. Moreover, we surmise that the sex (female for LβT2 samples, male for αT3-1 samples) and the developmental stage of each line may differentially affect their gene expression profiles, as previously shown in enriched primary mouse gonadotropes [42]; in addition, sex genes may have a major impact on a cell's biology (for review, see [43]). With respect to the sex of LβT2 cells, the original functional characterization report indicated that the clonal cell line was derived from male mice [16]. Our cytogenetic, genomic, RNA-seq, and ATAC-seq analyses are consistent with LβT2 cells originating from a female mouse. However, the possibility of a male mouse origin and loss of

chromosome Y cannot be excluded. Y chromosome loss has been described in human tumors as well as in a number of hepatocellular carcinoma cell lines [44] (for review, see [43]).

Our work demonstrates the existence of two genetically distinct LβT2 lines that have been distributed and used in the endocrine research field. Of note, LβT2a and LβT2b show different profiles of gene expression and gene responses to GnRH. Differences in patterns of gene expression and GnRH regulation could partially be attributed to variations in gene CN; gene or promoter mutations; alterations in the expression of transcription factors, transcriptional regulators, or upstream intracellular signaling molecules; variations in promoter methylation patterns and/or in chromatin/histone modifications; or different patterns of microRNA expression (for review, see [45]). Future epigenomic and chromatin accessibility studies may provide some insight into the underlying mechanisms.

Differential gene expression between the two LβT2 lines may also account for synthesis of different proteins, resulting in a different cell shape and size. Further, a larger exposed surface area, a lower nuclear/cytoplasmic ratio, and a more elongated shape may reflect functional dissimilarities between the lines. For instance, elongation of cell shape is known to augment plasma membrane signaling [46]. Cellular protrusions, as observed in LβT2b, are thought to enable highly specific cell-to-cell communication [47]. Interestingly, these protrusions vary in their diameter, length, cytoskeletal components, and function. Although further scrutiny is needed to characterize the protrusions used by LβT2b, the existence of signaling protrusions highlights their anticipated impact on cellular function.

Our results establish STR profiles that can be used to authenticate these gonadotrope cell lines. The surprising discovery that there are at least two LβT2 cell lines in circulation further underscores the importance of establishing genetic authentication standards. Although we focused on mouse gonadotrope cell lines in this study, the results have widespread implications relevant to the accuracy and reproducibility of biomedical research. These findings suggest that it is advisable to establish and monitor STR standard profiles for all cell lines used in research.

Acknowledgments

qPCR assays were carried out at the Quantitative PCR CoRE of the ISMMS. Sequencing assays were performed at the Molecular Cytogenetic Core of the Albert Einstein College of Medicine. Imaging was performed at the ISMMS Microscopy CoRE of the Icahn School of Medicine at Mount Sinai.

Financial Support: This work was supported by the National Institutes of Health (NIH) Grant DK46943 and the National Institute of Allergy and Infectious Diseases Grant U19 AI117873 (to S.C.S.). It was also supported by NIH P50 HD012303, R01 HD082567, R01 HD072754, P30 DK063491, P30 CA023100, and P42 ES010337 (to P.L.M.), as well as by the Canadian Institutes of Health Research Operating Grant MOP-123447 (to D.J.B.) and the Natural Sciences and Engineering Research Council of Canada Discovery Grant 2015-05178 (to D.J.B.). The authors declare that the research was conducted in the absence of any commercial or financial relationships that could be constructed as a potential conflict of interest.

Author Contributions: F.R.-Z. designed and conducted the experiments and analyzed and interpreted data. Y.G. contributed analytic tools and analyzed data. J.S., Y.S., N.H., K.K., C.M., P.N., and V.N. conducted experiments and analyzed data. H.P. analyzed and interpreted data and drafted the manuscript. C.T., D.J.B., and P.L.M. contributed materials. J.L.T. analyzed and interpreted data. S.C.S. conceived the research, analyzed the data, and edited the manuscript. All authors drafted or revised the work critically and approved the final version to be submitted.

Correspondence: Stuart C. Sealfon, MD, Icahn School of Medicine at Mount Sinai, Annenberg 14-44, Box 1137, One Gustave L. Levy Place, New York, New York 10029. E-mail: stuart.sealfon@mssm.edu.

Disclosure Summary: The authors have nothing to disclose.

References and Notes

1. RRID:CVCL_0149. https://scicrunch.org/resolver/CVCL_0149.
2. RRID:CVCL_0398. https://scicrunch.org/resolver/CVCL_0398.

3. Bernard DJ, Fortin J, Wang Y, Lamba P. Mechanisms of FSH synthesis: what we know, what we don't, and why you should care. *Fertil Steril*. 2010;**93**(8):2465–2485.
4. Bliss SP, Navratil AM, Xie J, Roberson MS. GnRH signaling, the gonadotrope and endocrine control of fertility. *Front Neuroendocrinol*. 2010;**31**(3):322–340.
5. Edwards BS, Clay CM, Ellsworth BS, Navratil AM. Functional role of gonadotrope plasticity and network organization. *Front Endocrinol (Lausanne)*. 2017;**8**:223.
6. Fortin J, Ongaro L, Li Y, Tran S, Lamba P, Wang Y, Zhou X, Bernard DJ. Minireview: Activin signaling in gonadotropes: what does the FOX say… to the SMAD? *Mol Endocrinol*. 2015;**29**(7):963–977.
7. Janjic MM, Stojilkovic SS, Bjelobaba I. Intrinsic and regulated gonadotropin-releasing hormone receptor gene transcription in mammalian pituitary gonadotrophs. *Front Endocrinol (Lausanne)*. 2017;**8**:221.
8. Naor Z. Signaling by G-protein-coupled receptor (GPCR): studies on the GnRH receptor. *Front Neuroendocrinol*. 2009;**30**(1):10–29.
9. Pincas H, Choi SG, Wang Q, Jia J, Turgeon JL, Sealfon SC. Outside the box signaling: secreted factors modulate GnRH receptor-mediated gonadotropin regulation. *Mol Cell Endocrinol*. 2014;**385**(1-2): 56–61.
10. Windle JJ, Weiner RI, Mellon PL. Cell lines of the pituitary gonadotrope lineage derived by targeted oncogenesis in transgenic mice. *Mol Endocrinol*. 1990;**4**(4):597–603.
11. Alarid ET, Windle JJ, Whyte DB, Mellon PL. Immortalization of pituitary cells at discrete stages of development by directed oncogenesis in transgenic mice. *Development*. 1996;**122**(10):3319–3329.
12. Choi SG, Jia J, Pfeffer RL, Sealfon SC. G proteins and autocrine signaling differentially regulate gonadotropin subunit expression in pituitary gonadotrope. *J Biol Chem*. 2012;**287**(25):21550–21560.
13. Graham KE, Nusser KD, Low MJ. LbetaT2 gonadotroph cells secrete follicle stimulating hormone (FSH) in response to active A. *J Endocrinol*. 1999;**162**(3):R1–R5.
14. Pernasetti F, Vasilyev VV, Rosenberg SB, Bailey JS, Huang HJ, Miller WL, Mellon PL. Cell-specific transcriptional regulation of follicle-stimulating hormone-β by activin and gonadotropin-releasing hormone in the LβT2 pituitary gonadotrope cell model. *Endocrinology*. 2001;**142**(6):2284–2295.
15. Thomas P, Mellon PL, Turgeon J, Waring DW. The L beta T2 clonal gonadotrope: a model for single cell studies of endocrine cell secretion. *Endocrinology*. 1996;**137**(7):2979–2989.
16. Turgeon JL, Kimura Y, Waring DW, Mellon PL. Steroid and pulsatile gonadotropin-releasing hormone (GnRH) regulation of luteinizing hormone and GnRH receptor in a novel gonadotrope cell line. *Mol Endocrinol*. 1996;**10**(4):439–450.
17. Kaiser UB, Conn PM, Chin WW. Studies of gonadotropin-releasing hormone (GnRH) action using GnRH receptor-expressing pituitary cell lines. *Endocr Rev*. 1997;**18**(1):46–70.
18. Almeida JL, Cole KD, Plant AL. Standards for cell line authentication and beyond. *PLoS Biol*. 2016; **14**(6):e1002476.
19. Stacey GN, Byrne E, Hawkins JR. DNA profiling and characterization of animal cell lines. *Methods Mol Biol*. 2014;**1104**:57–73.
20. Masters JR, Thomson JA, Daly-Burns B, Reid YA, Dirks WG, Packer P, Toji LH, Ohno T, Tanabe H, Arlett CF, Kelland LR, Harrison M, Virmani A, Ward TH, Ayres KL, Debenham PG. Short tandem repeat profiling provides an international reference standard for human cell lines. *Proc Natl Acad Sci USA*. 2001;**98**(14):8012–8017.
21. Ruf-Zamojski F, Ge Y, Nair V, Zamojski M, Pincas H, Toufaily C, Tome-Garcia J, Stoeckius M, Stephenson W, Smith GR, Bernard DJ, Tsankova NM, Hartmann BM, Fribourg M, Smibert P, Swerdlow H, Turgeon JL, Sealfon SC. Single-cell stabilization method identifies gonadotrope transcriptional dynamics and pituitary cell type heterogeneity. *Nucleic Acids Res*. 2018;**46**(21):11370–11380.
22. Stern E, Ruf-Zamojski F, Zalepa-King L, Pincas H, Choi SG, Peskin CS, Hayot F, Turgeon JL, Sealfon SC. Modeling and high-throughput experimental data uncover the mechanisms underlying *Fshb* gene sensitivity to gonadotropin-releasing hormone pulse frequency. *J Biol Chem*. 2017;**292**(23):9815–9829.
23. Almeida JL, Hill CR, Cole KD. Mouse cell line authentication. *Cytotechnology*. 2014;**66**(1):133–147.
24. Howe B, Umrigar A, Tsien F. Chromosome preparation from cultured cells [published online ahead of print 28 January 2014]. *J Vis Exp*. doi: 10.3791/50203.
25. Montagna C, Andrechek ER, Padilla-Nash H, Muller WJ, Ried T. Centrosome abnormalities, recurring deletions of chromosome 4, and genomic amplification of HER2/neu define mouse mammary gland adenocarcinomas induced by mutant HER2/neu. *Oncogene*. 2002;**21**(6):890–898.
26. Davisson MT; International Committee on Standardized Genetic Nomenclature for Mice. Rules and guidelines for nomenclature of mouse genes. *Gene*. 1994;**147**(2):157–160.
27. Knouse KA, Wu J, Hendricks A. Detection of copy number alterations using single cell sequencing [published online ahead of print 17 February 2017]. *J Vis Exp*. doi: 10.3791/55143.
28. RRID:SCR_003070. https://scicrunch.org/resolver/SCR_003070.

29. RRID:SCR_002798. https://scicrunch.org/resolver/SCR_002798.
30. Ruf-Zamojski F, Fribourg M, Ge Y, Nair V, Pincas H, Zaslavsky E, Nudelman G, Tuminello SJ, Watanabe H, Turgeon JL, Sealfon SC. Regulatory architecture of the LβT2 gonadotrope cell underlying the response to gonadotropin-releasing hormone. *Front Endocrinol (Lausanne)*. 2018;**9**:34.
31. Wurmbach E, Yuen T, Ebersole BJ, Sealfon SC. Gonadotropin-releasing hormone receptor-coupled gene network organization. *J Biol Chem*. 2001;**276**(50):47195–47201.
32. Wang Q, Chikina M, Zaslavsky E, Pincas H, Sealfon SC. β-catenin regulates GnRH-induced FSHβ gene expression. *Mol Endocrinol*. 2013;**27**(2):224–237.
33. Ruf-Zamojski F, Ge Y, Pincas H, Shan J, Song Y, Hines N, Kelley K, Montagna C, Nair P, Toufaily C, Bernard DJ, Mellon PL, Nair V, Turgeon JL, Sealfon SC. Supplemental data repository. figshare2019. Deposited 12 February 2019. https://figshare.com/s/8bc4444df6635d3f9aee.
34. Wang Y, Libasci V, Bernard DJ. Activin A induction of FSHβ subunit transcription requires SMAD4 in immortalized gonadotropes. *J Mol Endocrinol*. 2010;**44**(6):349–362.
35. Li B, Murphy KL, Laucirica R, Kittrell F, Medina D, Rosen JM. A transgenic mouse model for mammary carcinogenesis. *Oncogene*. 1998;**16**(8):997–1007.
36. Pernasetti F, Spady TJ, Hall SB, Rosenberg SB, Givens ML, Anderson S, Paulus M, Miller WL, Mellon PL. Pituitary tumorigenesis targeted by the ovine follicle-stimulating hormone β-subunit gene regulatory region in transgenic mice. *Mol Cell Endocrinol*. 2003;**203**(1-2):169–183.
37. Voelkel-Johnson C, Voeks DJ, Greenberg NM, Barrios R, Maggouta F, Kurtz DT, Schwartz DA, Keller GM, Papenbrock T, Clawson GA, Norris JS. Genomic instability-based transgenic models of prostate cancer. *Carcinogenesis*. 2000;**21**(8):1623–1627.
38. Sargent LM, Dragan YP, Sattler G, Xu YH, Wiley J, Pitot HC. Specific chromosomal changes in albumin simian virus 40 T antigen transgenic rat liver neoplasms. *Cancer Res*. 1997;**57**(16):3451–3456.
39. Ham J, Webster J, Bond JA, Jasani B, Lewis MD, Hepburn PJ, Davies JS, Lewis BM, Thomas DW, Scanlon MF. Immortalized human pituitary cells express glycoproteinα-subunit and thyrotropin β (TSH β). *J Clin Endocrinol Metab*. 1998;**83**(5):1598–1603.
40. Jin L, Kulig E, Qian X, Scheithauer BW, Eberhardt NL, Lloyd RV. A human pituitary adenoma cell line proliferates and maintains some differentiated functions following expression of SV40 large T-antigen. *Endocr Pathol*. 1998;**9**(2):169–184.
41. Stephens PJ, Greenman CD, Fu B, Yang F, Bignell GR, Mudie LJ, Pleasance ED, Lau KW, Beare D, Stebbings LA, McLaren S, Lin ML, McBride DJ, Varela I, Nik-Zainal S, Leroy C, Jia M, Menzies A, Butler AP, Teague JW, Quail MA, Burton J, Swerdlow H, Carter NP, Morsberger LA, Iacobuzio-Donahue C, Follows GA, Green AR, Flanagan AM, Stratton MR, Futreal PA, Campbell PJ. Massive genomic rearrangement acquired in a single catastrophic event during cancer development. *Cell*. 2011; **144**(1):27–40.
42. Qiao S, Nordström K, Muijs L, Gasparoni G, Tierling S, Krause E, Walter J, Boehm U. Molecular plasticity of male and female murine gonadotropes revealed by mRNA sequencing. *Endocrinology*. 2016;**157**(3):1082–1093.
43. Shah K, McCormack CE, Bradbury NA. Do you know the sex of your cells? *Am J Physiol Cell Physiol*. 2014;**306**(1):C3–C18.
44. Park SJ, Jeong SY, Kim HJ. Y chromosome loss and other genomic alterations in hepatocellular carcinoma cell lines analyzed by CGH and CGH array. *Cancer Genet Cytogenet*. 2006;**166**(1):56–64.
45. Bahrami S, Drabløs F. Gene regulation in the immediate-early response process. *Adv Biol Regul*. 2016; **62**:37–49.
46. Rangamani P, Lipshtat A, Azeloglu EU, Calizo RC, Hu M, Ghassemi S, Hone J, Scarlata S, Neves SR, Iyengar R. Decoding information in cell shape. *Cell*. 2013;**154**(6):1356–1369.
47. Buszczak M, Inaba M, Yamashita YM. Signaling by cellular protrusions: keeping the conversation private. *Trends Cell Biol*. 2016;**26**(7):526–534.